Supporting Information

Synthesis and Substitution Chemistry of Redox-Active Manganese/Cobalt Oxide Nanosheets

Nobuyuki Sakai,[*,†] Katsutoshi Fukuda,[‡] Renzhi Ma,[†] and Takayoshi Sasaki[*,†]

[†] International Center for Materials Nanoarchitectonics (WPI-MANA), National Institute for Materials Science (NIMS), 1-1 Namiki, Tsukuba, Ibaraki 305-0044, Japan.

[‡] Office of Society-Academia Collaboration for Innovation, Kyoto University, Yoshida-honmachi, Sakyo-ku, Kyoto 606-8501, Japan.

* Corresponding author: (N.S.) sakai.nobuyuki@nims.go.jp

* Corresponding author: (T.S.) sasaki.takayoshi@nims.go.jp

Table S1. Refinement data for XRD patterns of Na-$Mn_{1-x}Co_xO_2$.

	x = 0.2		x = 0.3		x = 0.4		x = 0.5	
hkl	d_{calc} (Å)	d_{obs} (Å)	d_{calc} (Å)	d_{obs} (Å)	d_{calc} (Å)	d_{obs} (Å)	d_{calc} (Å)	d_{obs} (Å)
003	5.65130	5.65423	5.64133	5.63991	5.62101	5.61150	5.61975	5.62567
006	2.82565	2.82559	2.82066	2.82211	2.81050	2.81346	2.80987	2.81346
101	2.45441	2.45454	2.44315	2.44293	2.43102	2.43144	2.42025	2.42132
102	2.38071	2.38050	2.37018	2.36962	2.35860	2.35765	2.34873	2.35053
104	2.14086	2.14071	2.13247	2.13107	2.12258	2.12342	2.11529	2.11489
105	2.00202	2.00193	1.99472	1.99525	1.98572	1.98450	1.97969	1.98039
107	1.73293	1.72818	1.72743	1.72636	1.72003	1.71855	1.71601	1.71497
108	1.61127	1.61124	1.60646	1.60763	1.59973	1.60047	1.59645	1.59743
110	1.43214	1.43091	1.42548	1.42585	1.41837	1.41891	1.41196	1.41168
113	1.38826	1.38832	1.38204	1.38181	1.37526	1.37149	1.36940	1.36938

Table S2. Valence, Ionic Radii, and Interatomic Distance for the Obtained Layered Crystals of Na-$Mn_{1-x}Co_xO_2$.

sample	N_{Mn}	N_{Co}	Z_{mean}	Z_{Co} [a]	Z_{Mn} [b]	r_{Mn} (Å) [c]	r_{mean} (Å) [d]	R_{M-O} (nm) [e]	a (nm) [f]
$x = 0.2$	0.81	0.19	3.50	3	3.62	0.574	0.569	0.1929	0.2859(2)
$x = 0.3$	0.72	0.28	3.52	3	3.72	0.562	0.557	0.1917	0.2846(3)
$x = 0.4$	0.62	0.38	3.53	3	3.85	0.547	0.546	0.1906	0.2829(3)
$x = 0.5$	0.52	0.48	3.48	3	3.92	0.539	0.542	0.1902	0.28229(5)
$K_{0.45}MnO_2$	1	0	3.55	–	3.55	0.582	0.582	0.1942	0.2879(2) [g]

[a] Valence of Co, Z_{Co}, is assumed to be 3 on the basis of XANES data. [b] Values obtained from $Z_{mean} = x \cdot Z_{Co} + (1-x) \cdot Z_{Mn}$. [c] Mean ionic radius of Mn^{4+} and Mn^{3+} (high spin state), r_{Mn}, is calculated as $r_{Mn} = (Z_{Mn} - 3) \cdot r_{Mn(IV)} + (4 - Z_{Mn}) \cdot r_{Mn(III, HS)}$. $r_{Mn(IV)} = 0.53$ Å and $r_{Mn(III, HS)} = 0.645$ Å.[S1] [d] Mean ionic radius of Mn and Co, r_{mean}, is calculated as $r_{mean} = x \cdot r_{Co(III, LS)} + (1-x) \cdot r_{Mn}$. $r_{Co(III, LS)} = 0.545$ Å.[S1] [e] Interatomic distance between metal ions and oxygen, R_{M-O}, is obtained as $R_{M-O} = r_{mean} + r_O$. $r_O = 1.36$ Å.[S1] [f] Values from Fig. 2. [g] Lattice constant a for $K_{0.45}MnO_2$ from ref. S2.

Table S3. Refinement data for XRD patterns of H-$Mn_{1-x}Co_xO_2$.

	$x = 0.2$		$x = 0.3$		$x = 0.4$		$x = 0.5$	
hkl	d_{calc} (Å)	d_{obs} (Å)	d_{calc} (Å)	d_{obs} (Å)	d_{calc} (Å)	d_{obs} (Å)	d_{calc} (Å)	d_{obs} (Å)
003	7.22223	7.22532	7.17688	7.17858	6.94558	6.97557	6.91473	6.93202
006	3.61111	3.61014	3.58844	3.59006	3.47279	3.46094	3.45736	3.45039
101	2.43843	2.44679	2.43866	2.44037	2.43923	2.44037	2.44080	2.43909
102	2.39338	2.39149	2.39304	2.39026	2.39058	2.39026	2.39164	2.39026
104	2.23531	2.23613	2.23323	2.22977	2.22156	2.22030	2.22105	2.21925
105	2.13538	2.13299	2.13238	2.12628	2.11596	2.11395	2.11464	2.11301
107	1.92297	1.89385	1.91849	1.92024	1.89447	1.93880	1.89185	1.88720
108	1.81853	1.83160	1.81353	1.81252	1.78692	1.78080	1.78384	1.78015
110	1.41683	1.41700	1.41708	1.41738	1.41804	1.41776	1.41905	1.41891
113	1.39033	1.39160	1.39024	1.39014	1.38938	1.38941	1.39008	1.39050

Table S4. Valence, Ionic Radii, and Interatomic Distance for the Obtained Layered Crystals of H-$Mn_{1-x}Co_xO_2$.

sample	N_{Mn}	N_{Co}	Z_{mean}	Z_{Co} [a]	Z_{Mn} [b]	r_{Mn} (Å) [c]	r_{mean} (Å) [d]	R_{M-O} (nm) [e]	a (nm) [f]
$x = 0.2$	0.82	0.18	3.75	3	3.91	0.540	0.541	0.1901	0.28335(3)
$x = 0.3$	0.72	0.28	3.66	3	3.92	0.540	0.541	0.1901	0.2833(1)
$x = 0.4$	0.62	0.38	3.55	3	3.89	0.543	0.544	0.1904	0.28346(9)
$x = 0.5$	0.53	0.47	3.50	3	3.94	0.537	0.541	0.1901	0.2836(1)
$H_{0.13}MnO_2$	1	0	3.87	–	3.87	0.545	0.545	0.1905	0.2842(8) [g]

[a] Valence of Co, Z_{Co}, is assumed to be 3 on the basis of XANES data. [b] Values obtained from $Z_{mean}=x\cdot Z_{Co}+(1-x)\cdot Z_{Mn}$. [c] Mean ionic radius of Mn^{4+} and Mn^{3+} (high spin state), r_{Mn}, is calculated as $r_{Mn}=(Z_{Mn}-3)\cdot r_{Mn(IV)}+(4-Z_{Mn})\cdot r_{Mn(III,\,HS)}$. $r_{Mn(IV)}$ = 0.53 Å and $r_{Mn(III,\,HS)}$ = 0.645 Å.[S1] [d] Mean ionic radius of Mn and Co, r_{mean}, is calculated as $r_{mean}=x\cdot r_{Co(III,\,LS)}+(1-x)\cdot r_{Mn}$. $r_{Co(III,\,LS)}$ = 0.545 Å.[S1] [e] Interatomic distance between metal ions and oxygen, R_{M-O}, is obtained as $R_{M-O}=r_{mean}+r_O$. r_O = 1.36 Å.[S1] [f] Values from Fig. 2. [g] Lattice constant a for $H_{0.13}MnO_2$ from ref. S3.

Table S5. Comparison of the values of Mn valence after protonation deduced from the dissolved amount of Co^{2+} ions and the investigation by titration and XANES.

sample	Z_{Mn} (before protonation) [a]	$Co^{2+}_{dissolved}$ [b]	Z_{Mn}' (after protonation) [c]	Z_{Mn} (after protonation) [d]
$x = 0.2$	3.62	11.6 mol%	3.86	3.91
$x = 0.3$	3.72	7.5 mol%	3.89	3.92
$x = 0.4$	3.85	2.6 mol%	3.92	3.89
$x = 0.5$	3.92	0.6 mol%	3.94	3.94

[a] Values from Table S1. [b] Values from Fig. S4. [c] Valence for Mn deduced from the dissolved amount of Co^{2+} and Z_{Mn} before protonation on the assumption that the same amount of Mn^{2+} is also dissolved as Co^{2+}, and Co^{4+} takes one electron from Mn^{3+} forming of Co^{3+} and Mn^{4+}. [d] Values from Table S2, which is estimated from the titration and XANES studies.

Table S6. Atomic concentration of $Mn_{1-x}Co_xO_2$ nanosheets revealed by XPS survey spectra.

sample	C 1s	N 1s	O 1s	Si 2p	Mn 2p	Co 2p	Mn : Co
$x = 0.0$	24.6%	0.9%	40.9%	29.4%	4.2%	ND	–
$x = 0.2$	41.4%	1.2%	32.9%	16.5%	6.3%	1.7%	0.8 : 0.22
$x = 0.3$	32.9%	1.0%	37.6%	18.3%	7.1%	3.1%	0.7 : 0.31
$x = 0.4$	34.1%	0.9%	37.6%	16.5%	6.6%	4.3%	0.6 : 0.39
$x = 0.5$	47.5%	1.2%	28.2%	19.1%	2.0%	2.0%	0.5 : 0.50

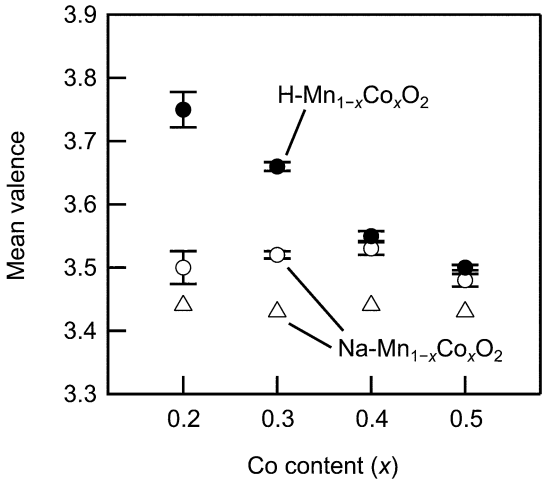

Figure S1. Mean valence of metal ions in the Na-$Mn_{1-x}Co_xO_2$ (open symbols) and H-$Mn_{1-x}Co_xO_2$ (closed symbols) powders estimated by chemical titration (circles) or Na content revealed by ICP measurement (triangles).

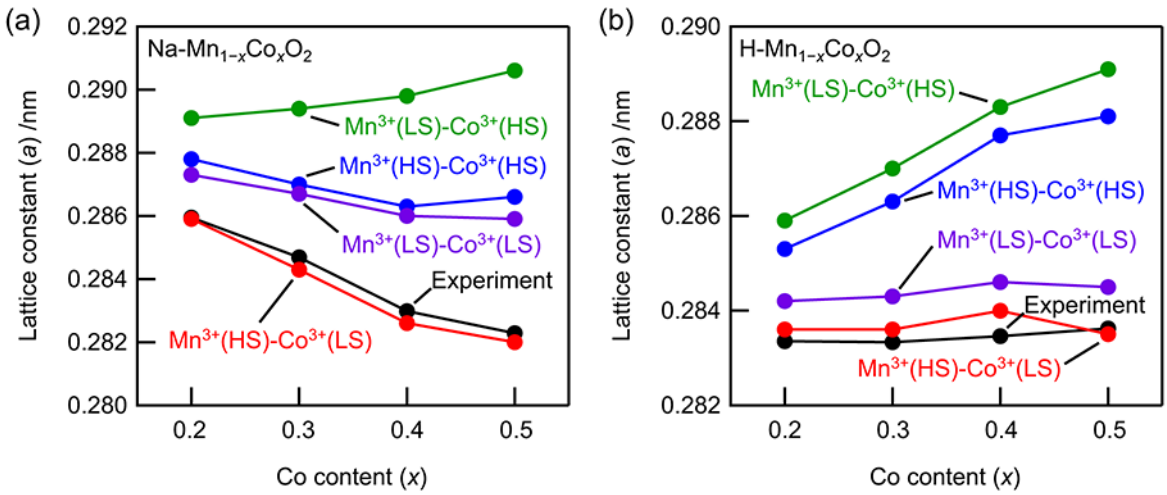

Figure S2. Calculated lattice constant *a* of (a) Na-$Mn_{1-x}Co_xO_2$ and (b) H-$Mn_{1-x}Co_xO_2$ on the basis of the bond length of (Mn/Co)–O estimated from Mn/Co ratio, Z_{Mn}, and ionic radii of O^{2-}, Mn^{4+}, Mn^{3+} and Co^{3+} in high spin state (HS) or low spin state (LS). The ratio of the lattice constant *a* to the bond length is assumed to be the same as that for (a) $K_{0.45}MnO_2$ (Table S1) or (b) $H_{0.13}MnO_2$ (Table S2). The plots of red in color are well consistent to the experimental data, suggesting that it is reasonable to assume high spin Mn^{3+} and low spin Co^{3+} ions in both samples, Na-$Mn_{1-x}Co_xO_2$ and H-$Mn_{1-x}Co_xO_2$. The plots of blue, green, and purple in color are obtained by considering other combinations including Mn^{3+}(HS)-Co^{3+}(HS), Mn^{3+}(LS)-Co^{3+}(HS), and Mn^{3+}(LS)-Co^{3+}(LS). The radii of Mn^{3+}(LS) and Co^{3+}(HS) are 0.58 Å and 0.61 Å, respectively.[S1]

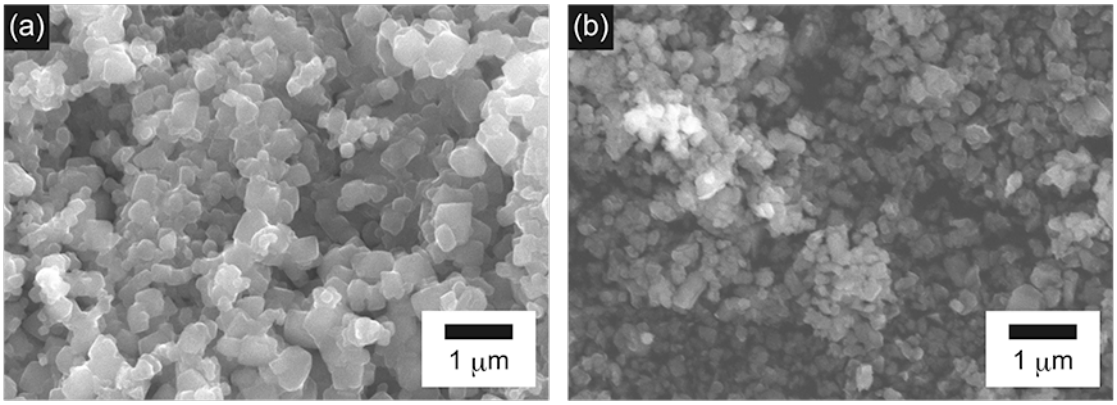

Figure S3. Typical SEM images of (a) Na-$Mn_{1-x}Co_xO_2$ and (b) H-$Mn_{1-x}Co_xO_2$ ($x = 0.2$) powders.

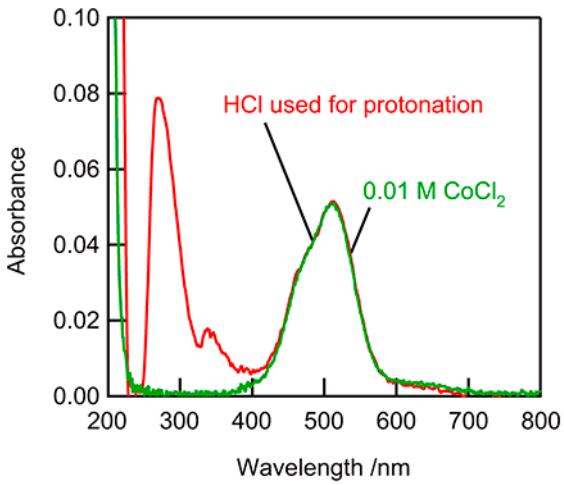

Figure S4. UV–vis absorption spectra of used 0.1 M HCl solution collected after the protonation process of Na-$Mn_{1-x}Co_xO_2$ (x = 0.2, red line) and fresh 0.1 M HCl containing 0.01 M $CoCl_2$ (green line). On the basis of absorption peak at 510 nm (ε = 5.1 mol^{-1} dm^3 cm^{-1} for Co^{2+}), it was estimated that 11.6 mol% of Co in the Na-$Mn_{1-x}Co_xO_2$ (x = 0.2) was dissolved as Co^{2+} ions. In a similar way, it was found that 7.5 mol%, 2.6 mol%, 0.6 mol% of Co in the Na-$Mn_{1-x}Co_xO_2$ (x = 0.3, 0.4, 0.5) was dissolved during the protonation process.

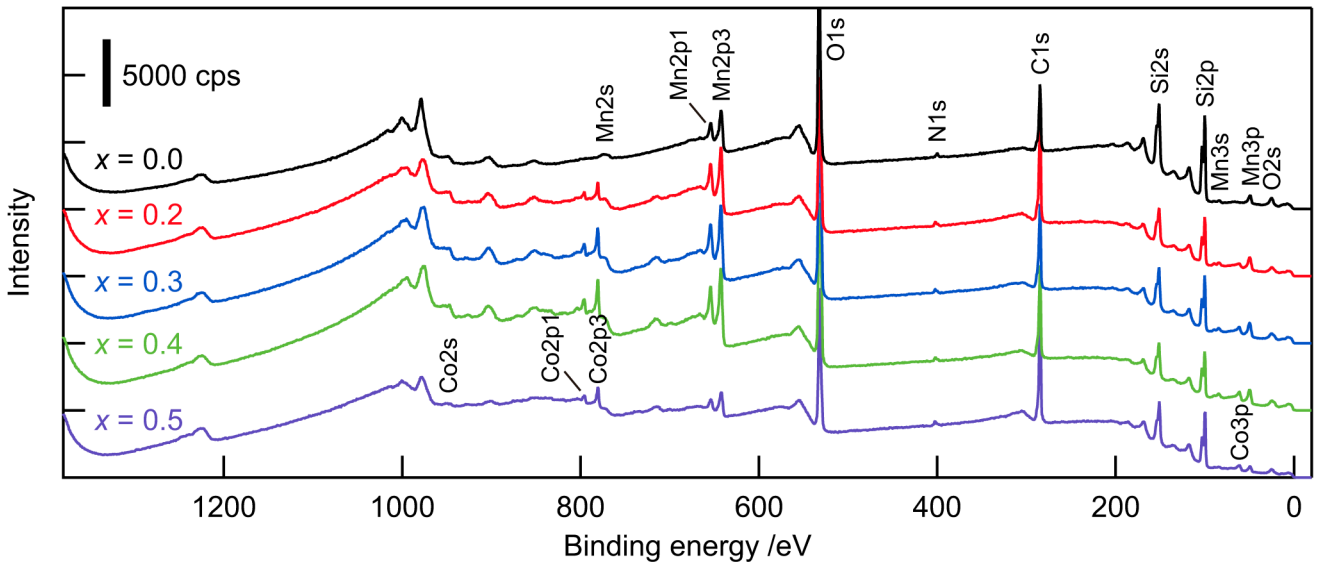

Figure S5. XPS spectra of nanosheets deposited on Si substrates coated with poly(diallyldimethylammonium) ions. The spectra were calibrated relative to the C 1s binding energy at 285.0 eV.

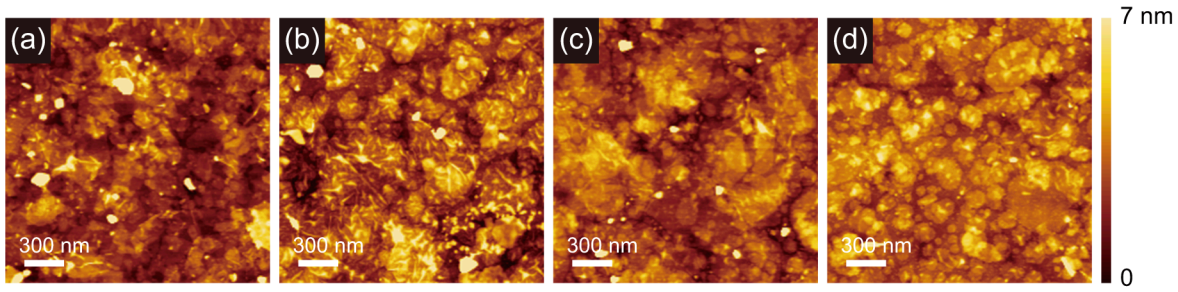

Figure S6. AFM images of $Mn_{1-x}Co_xO_2$ nanosheets deposited on flat ITO substrates (Kuramoto Co., Ltd.) pre-coated with PEI: (a) $x = 0.2$, (b) $x = 0.3$, (c) $x = 0.4$, (d) $x = 0.5$.

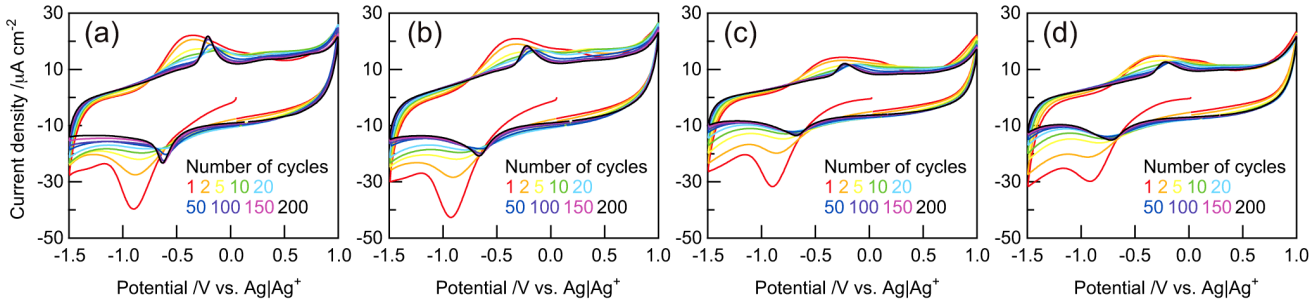

Figure S7. Changes of cyclic voltammogram of monolayer films of $Mn_{1-x}Co_xO_2$ nanosheet electrodes as a function of number of cycles in a propylene carbonate solution containing 0.1 mol dm^{-3} $LiClO_4$ at a sweep rate of 50 mV s^{-1}: (a) $x = 0.2$, (b) $x = 0.3$, (c) $x = 0.4$, (d) $x = 0.5$.

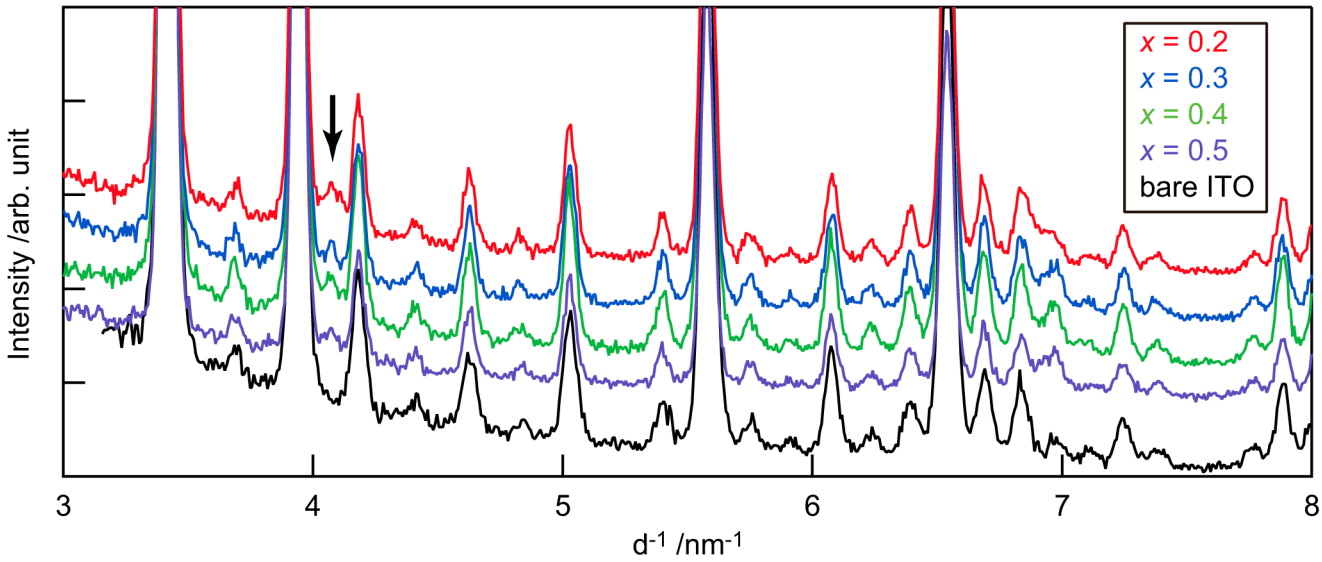

Figure S8. In-plane XRD patterns of monolayer films of $Mn_{1-x}Co_xO_2$ (x = 0.2, 0.3, 0.4, 0.5) nanosheet electrodes after 200 cycles of potential sweeps. The arrow indicates the peak corresponding to 10 reflection of the nanosheets. All other peaks are ascribable to ITO substrates.

References

(S1) Shannon, R. D. Revised Effective Ionic Radii and Systematic Studies of Interatomic Distances in Halides and Chalcogenides. *Acta Cryst. A* **1976**, *32*, 751–767.

(S2) Omomo, Y.; Sasaki, T.; Wang, L. Z.; Watanabe, M. Redoxable Nanosheet Crystallites of MnO_2 Derived via Delamination of a Layered Manganese Oxide. *J. Am. Chem. Soc.* **2003**, *125*, 3568–3575.

(S3) Fukuda, K.; Nakai, I.; Ebina, Y.; Tanaka, M.; Mori, T.; Sasaki, T. Structure Analysis of Exfoliated Unilamellar Crystallites of Manganese Oxide Nanosheets. *J. Phys. Chem. B* **2006**, *110*, 17070–17075.